RSC Advances

ROYAL SOCIETY OF CHEMISTRY

www.rsc.org/advances

ToC figure: The formation of iron oxide NPs in scaled-up conditions is monitored in situ using a handled magnetic portable sensor.

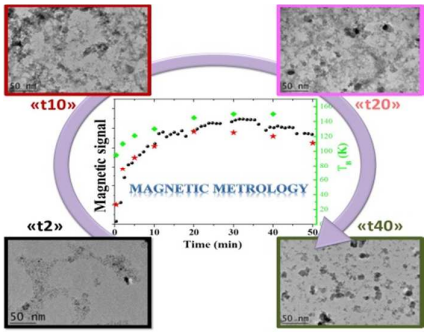

Cite this: DOI: 10.1039/c0xx00000x

www.rsc.org/xxxxxx

ARTICLE TYPE

Magnetic Metrology for iron oxide nanoparticles scaled-up synthesis

Irena Milosevic[a], Fabienne Warmont[b], Yoann Lalatonne[a] and Laurence Motte[a*]

Received (in XXX, XXX) Xth XXXXXXXXX 20XX, Accepted Xth XXXXXXXXX 20XX
DOI: 10.1039/b000000x

The evolution of magnetic properties during the formation of iron oxide NPs by co-precipitation in aqueous media and in scaled-up conditions is monitored in situ using a handled portable sensor measuring magnetic signal that is proportional to third derivative of magnetization. A detailed tracking of subsequent changes is also performed ex situ using more conventional analytical and physical methods.

Iron oxide NPs are highly exciting nanomaterials both from fundamental research point of view considering the dependence of the magnetic properties with size, shape, composition, surface and interaction, and for their numerous potential applications in bio- and nanotechnologies ranging from diagnosis, therapies, in medical care to data storage in electronics or as catalytic materials[1-5]. For such applications, the scale up of lab bench NPs synthesis to gram-scale or kilogram-scale synthesis of size-controlled iron oxide NPs is of key importance. The synthesis in aqueous media by co-precipitation of ferrous and ferric salts includes a number of advantages compared to other chemical methods. Among them are the extremely low cost, the possibility of working with mild temperature conditions, the absence of toxic byproducts and the possibility of obtaining large amount of NPs. Moreover these water soluble NPs are easily surface tailored to impart specific properties to the material[2,6]. Recently, it has been shown that the nucleation and growth of magnetite, formed by aqueous co-precipitation, proceeds through the rapid agglomeration of nanometric primary particles (2 nm)[7]. Primary particles, consisting of iron (hydr)oxide, arise from the interaction of Fe(II) with ferrihydrite hydrogel and are formed 2 min after the initial addition of iron chloride to the base. These primary particles aggregate in branched networks and with time generated spheroidal NPs of 5-15nm. With further reaction time, the NPs grew in number and size at the expense of the primary particles. The final size could be affected by several parameters, such as the pH and ionic strength of solution, reaction temperature, Fe(II)/Fe(III) ratio, the nature of precursor salts and base and reagents flow rate and mixing time[8-10]. These various parameters could explain that commercially available NPs, prepared using the precipitation method, present significant batch to batch performance differences[11]. This is also related to the fact that the formation of iron oxide NPs is a very fast process[10, 12-13], and that no sensitive, standardized easy to use measurement techniques exist for the validation and quality control of this synthesis. Finally, despite the considerable number of publications on the synthesis of iron oxide NPs, there is still lack of reports dealing with the magnetic properties evolution at different points of the synthesis from the same initial precursor solution. This should lead to the optimization of iron oxide NPs synthesis with controllable and reproducible process, and should allow to progress towards good manufacturing practice standards and towards regulatory approval (e.g. by FDA US Food and Drug Administration) for biomedical and healthcare use.

Here we study the nucleation and growth mechanism of iron oxide NPs formed by water co-precipitation, scaled-up for industrial production, using an innovative magnetic device (called MIAtek), measuring the third derivative of the magnetization around zero field[14]. Consequently, this sensor is very sensitive to superparamagnetic (SPM) or weakly ferromagnetic (small coercive field) NPs behavior at room temperature. In previous works, we have shown that the MIA technologies, firstly devoted to magnetic immunoassays[15], feature sensitivity, rapidity and ease of use compared to conventional magnetic ones (e.g. superconducting quantum interference device (SQUID) or Vibrating Sample Magnetometer (VSM) in order to characterize the magnetic properties of the synthesized nanomaterial or to quantitatively monitor in situ NP cell internalization[16-18]. This work shows the suitability of MIAtek to achieve in situ metrological monitoring of iron oxide NPs synthesis in aqueous media and at a pilot scale. Detailed tracking of subsequent changes is performed using both MIAtek and more conventional analytical and physical methods: TEM, DLS and VSM. In addition to the work of Baumgartner et al.[7], we showed that the primary particles present SPM behavior. The set of results provides valuable information that can be used either to improve existing preparation methodologies or elaborate new ones, more appropriate for volume production.

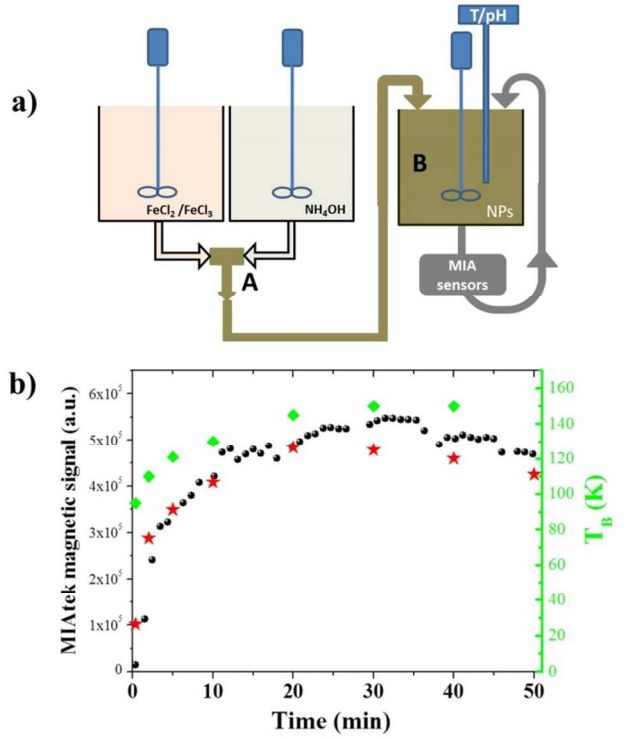

Fig.1 a) Scheme of the laboratory two-stage continuous flow reactor. A, B are nucleation and growth reactor respectively. b) Typical time series of the nucleation and growth process followed with MIAtek reader. Black points and red stars are in situ and ex situ aliquoted samples MIAtek measurements respectively. Green diamonds are the blocking temperature values of the aliquoted samples

The iron oxide NPs synthesis is performed within controlled physicochemical conditions scalable for industrial level production (see Experimental Section). Briefly, NPs are prepared in a laboratory two-stage continuous flow reactor, Figure 1.a. The ammonium hydroxide and iron chloride solutions (Fe(II)/Fe(III)=1/2) are mixed at constant inflow in first reactor (nucleation reactor) and NPs growth process is performed in second reactor stage (growth reactor). Magnetic measurements are recorded using handled portable MIAtek reader and performed at the nucleation reactor outlet (sample labeled "t0") and in situ and continuously at the second reactor outlet, Figure 1.a. The first acquisition in the growth reactor is performed 2 min after nucleation stage up to 40 min, with an acquisition interval of 1 min. Moreover, the reaction mixture was aliquoted and frozen at different reaction times and collected samples were then characterized "ex-situ" using MIAtek, VSM, DLS and TEM. Iron content was estimated by Inductively Coupled Plasma Mass Spectrometry (ICP-MS) analysis.

Figure 1.b shows a typical time series of the nucleation and growth process followed with MIAtek (black points). Red stars correspond to ex-situ MIAtek acquisition of the aliquoted samples. A good correlation between in-situ and ex-situ signals is observed. This indicates that collected samples are representative of the reaction time events validating that more conventional methods (DLS, MET and VSM) can be used to investigate the sequence of morphological, structural and magnetic changes taking place during the NP precipitation. Surprisingly, at the early stage of the reaction, sample "t0", a magnetic signal is already detected, indicating SPM behavior. With time, the magnetic signal increases until a plateau, after 20 min, is observed. Therefore, iron oxide NPs are generated through the nucleation and growth of SPM primary particles. Moreover, after 20 min and up to 2 hours, no significant differences in magnetic signal occurs (Supplementary Figure S1). Considering that the variation of magnetic properties variation is correlated mainly to the size evolution and magnetic dipolar interactions, this seems to indicate that optimal size is achieved and the end of the reaction is after about 20 min. This is in accordance with iron yields measured with ICPMS, as in Table 1, showing that the reaction is complete within 20-30 min.

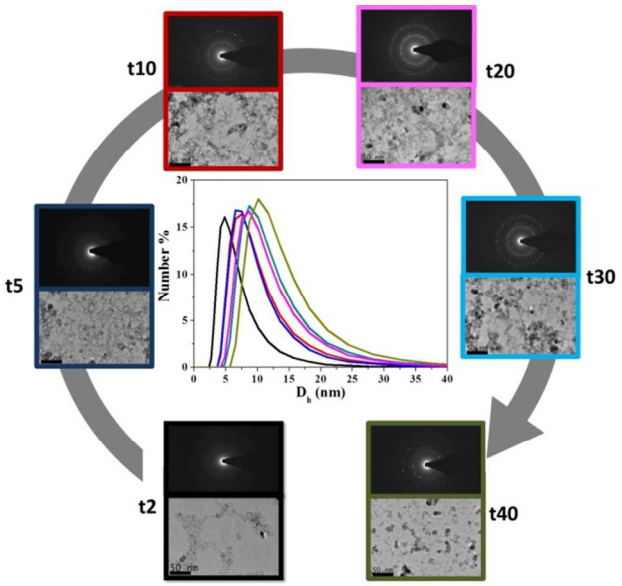

Fig.2 Evolution of the characteristic hydrodynamic diameters (D_h), TEM and electron diffraction images between 2 and 40 minutes**.**

Figure 2 shows the evolution of the characteristic hydrodynamic diameters (D_h), TEM and electron diffraction patterns obtained for time aliquoted samples (Supplementary Figure S2). The average D_h increases with the reaction time from 6 nm to 12 nm. Concomitantly, the full width at half maximum of the D_h distribution increases, as shown in Table 1. The TEM sample "t2" is characterized by branched network of very small particles (≈3-4 nm), not well crystallized, but not amorphous. Within further reaction time, the network disappears to finally obtain predominantly well crystallized iron oxide nanoparticles with an average size of about 7 nm. The diffraction patterns show the evolution of the NP cristallinity. The number of "final" NPs increases with time at the expense of the branched network. Considering the various step rule scenarios presented in Baumgartener publication[7], our experimental conditions are in accordance with their considerations relating to the phase transformation occurring from rapid agglomeration of nanometric ferrihydrite primary particles without formation of intermediate amorphous bulk precursor phase. Hence, the estimated ratio of free energy gain per unit volume (g_i) on formation of ferrihydrite (Fh) versus magnetite (Mt) nuclei formation (g_{Fh}/g_{Mt}) is in the range of 0,7-0,94 (see supplementary information for detailed calculation). Considering a range for surface energy ratio γ_{Fh}/γ_{Mt} = 0.25-0.5, this corresponds to the boundary window (stability) for which the formation of ferrihydrite primary particles is favored and induce magnetite nucleation and growth. In addition, our work shows that these primary particles present SPM behavior as characterized with MIAtek (Figure1.b) and highlight

below with VSM measurements.

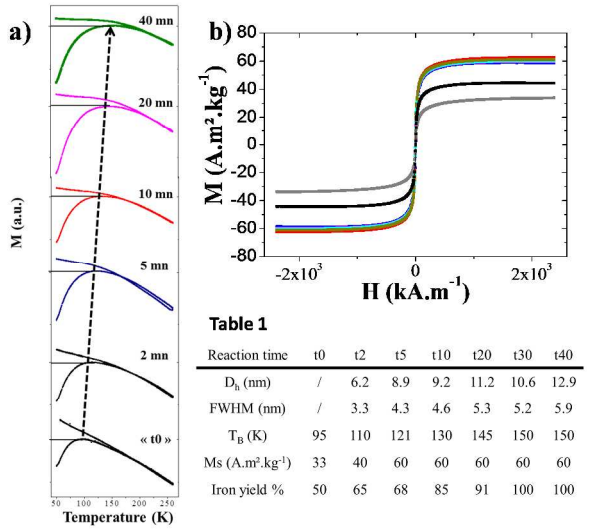

Table 1

Reaction time	t0	t2	t5	t10	t20	t30	t40
D_h (nm)	/	6.2	8.9	9.2	11.2	10.6	12.9
FWHM (nm)	/	3.3	4.3	4.6	5.3	5.2	5.9
T_B (K)	95	110	121	130	145	150	150
Ms ($A.m^2.kg^{-1}$)	33	40	60	60	60	60	60
Iron yield %	50	65	68	85	91	100	100

Fig.3 a) Ex situ characterizations. A. Zero field cooled and field cooled magnetizations curves, b) Hysteresis M(H) at 300 K, Table 1. Properties of NP sample: hydrodynamic diameters (D_h), full width at half maximum (FWHM), blocking temperatures (T_B), saturation magnetization (M_s) at 300K and iron yield.

Figure 3 a depicts magnetization vs. temperature curves after zero field cooling (ZFC) and after field cooling (FC) measured at 100 Oe for the various aliquoted samples. All of the samples show SPM behavior[19-21], i.e. showing for ZFC curve a gradual increase of the magnetization until blocking temperature T_B and for higher temperatures a 1/T Curie-type decrease. Furthermore, the FC curve overlaps with the ZFC curve for high temperatures and then splits from the ZFC curve due to remanent magnetization acquired by particles while blocking in an external field. The magnetizations in ZFC curves have been normalized to the blocking temperature and are reported as green diamonds in Figure 1.b and in Table 1.

A T_B increase is observed continuously with time, from 95 K to 145 K and after 30 min, a constant value 150 K is measured. Such an increase in TB has to be correlated to the increase of the NP diameter, as in Table 1. The temperature dependence in FC curves below T_B characterizes the particle interactions: the flatter, the stronger the interactions. Therefore, after 20 min, the NPs (average size = 7 nm) present stronger particle interactions than the smaller ones grown at shorter time. Considering NP size evolution, the higher T_B value in ZFC curves are observed for larger NPs and the relative peak broadening in ZFC curves shows the distribution of energy barriers (E_B) for spin freezing. The energy barrier includes the magnetic anisotropy energy related to particle size and the dipole–dipole interaction energy depending on the inter-particle distance in each sample. This latter parameter is directly correlated to the iron reaction yield which increases with time, as in Table 1. The hysteresis loops of the various aliquots at 300 K are shown in Figure 3.b. All samples exhibit reversible sigmoidal magnetization curve characteristic of SPM behavior. The saturation magnetization M_s increases with time from 30 up to 60 Am^2kg^{-1} until a plateau is observed at about 20 min (Fig. 3.b and Table 1). M_s values are close to those reported for magnetite or maghemite NPs prepared by similar method[22-25].

Due to the presence of oxygen in the headspace of reactors, in the course of the synthesis, magnetite is oxidized and maghemite or mixed magnetite/maghemite are formed. The increase of Ms along with particle size has been reported in numerous publications and can be prevalently related with the inter-particle interaction that depends on particle size, inter-particle spacing, and the presence of a spin disorder layer on NP surface [16,26-27].

As previously discussed, primary particles (sample "t0") were considered in the first approximation as ferrihydrite NPs based on TEM characterization (Fig. 3) and the publication of Baumgartener et al.[7]. In another work, the publication of Guyodo et al. reported SPM behavior at room temperature for ferrihydrite samples with an average size between 3 to 5.5 nm[28]. The T_B and M_s (300 K) values are in the range of 45K to 80 K and 6 to 13 Am^2kg^{-1} respectively. In our case, T_B and M_s values for sample "t0" are 95K and 33 Am^2kg^{-1}. This indicates that sample "t0" cannot be pure ferrihydrite NPs. On the other hand, Song et al. showed that magnetite NPs, with an average size of 3 nm and 5 nm, are characterized by T_B and M_s values of 40 K , 56 Am^2kg^{-1}, and 96 K, 59 Am^2kg^{-1} respectively[26]. Moreover, maghemite NPs with size distribution from 3 to 5 nm exhibit T_B and M_s values of 94 K and 30 Am^2kg^{-1} [29]. On the basis of these different works and our own results, this suggests that the sample "t0" is a mixture of ferrihydrite and maghemite phases.

Conclusions

Our work shows an original approach to valid routine monitoring and quality control of iron oxide NP synthesis using MIAtek. With this sensor and for a complete metrology approach, it is necessary in the first step to fully characterize the material properties such as size, concentration, magnetic behavior (T_B, M_s, H_c, for SPM or slightly ferromagnetic NPs) with conventional techniques. This first step defines the standard for a specific synthesis. Hence, the reproducibility of the MIAtek signal under the same experimental conditions allows validating the quality of the process and physical-chemical NP characteristics. Evidently, a change in the experimental conditions could lead to new NP properties and so a new standard would be generated. In this work, we used classical iron oxide co-precipitation in aqueous media as a proof of concept for such innovative magnetic metrology. We thus anticipate our approach to be a possible starting point to extent to other SPM or weakly ferromagnetic NPs synthesis.

Notes and references

[a] *Université Paris 13, Sorbonne Paris Cité, Laboratoire CSPBAT, CNRS, UMR 7244, 74 avenue M. Cachin 93017 Bobigny, E-mail: Laurence.motte@univ-paris13.fr*

[b] *CRMD, UMR 6619 CNRS, 1b rue de la Férollerie 45 071 Orléans , France*

† Electronic Supplementary Information (ESI) available: Typical time series of the nucleation and growth process followed with MIAtek reader for longer reaction time, Calculation of boundary window for estimated ranges for surface and bulk-energy ratio for Fh/Mt stability and TEM images with high magnification of the various aliquoted samples. See DOI: 10.1039/b000000x/

‡ Experimental Section

Iron oxide nanoparticles synthesis: NPs were prepared by a coprecipitation method at a pilot scale by addition (0.0144 mol.min^{-1}) of an ammonium hydroxide solution (0.36 mol.L^{-1}) with an iron chloride solution ([Fe] = 0.12 mol.L^{-1} with a stoichiometric ratio Fe(II)/Fe(III) = ½). The entire process is thermostated at 30°C and the pH and magnetic signal were measured at regular time intervals in the growth reactor (see Figure 1).

Ex-situ Characterization techniques: Ten milliliters samples were taken from the reaction mixture at different times (2, 5, 10, 20, 30, 40, 50 minutes) and rapidly frozen in liquid nitrogen in order to stop the growth of nanoparticles. Obtained particles were washed several times by magnetic decantation with deionized water. Each time, supernatant was discarded, and the final precipitate was finally dispersed in water at pH = 2.

The magnetism of collected samples was characterized using a vibrating sample magnetometer, VSM (Quantum Design, Versalab) and MIAtek (ex-situ) at room temperature. Measurements were performed on liquid samples. The magnetization curve was obtained with VSM by cycling the applied field from -2300 to +2300 kA.m^{-1} for two times with a step rate of 8 kA.s^{-1} and the temperature was set to 300 K. The ZFC curve is obtained by first cooling the system in zero field from 270 K to 50 K. Next, the field is applied and subsequently the magnetization is recorded while increasing the temperature gradually. The FC curve is measured by decreasing the temperature in the same applied field.

Bright field imaging and electron diffraction studies were carried out with a Philips CM20 microscope operating at 200 kV. The samples were prepared by dispersing NPs in ethanol then depositing it onto a carbon film supported by a copper grid.

The hydrodynamic diameter and the zeta potential of nanoparticles were determined by dynamic laser light scattering (DLS) on a Nano-ZS ZEN 3600 device (Malvern Instruments, Malvern, UK).

Determination of iron content was performed by Inductively Coupled Plasma Mass Spectrometry (ICP-MS) analysis (Agilent 7500ce). The samples were digested in concentrated HNO_3 solution and diluted with a 2% HNO_3 solution for analysis.

Acknowledgements

We thank L. Lenglet for discussion, Neelogy company and FUI grant (project 3MT) for providing scale- up laboratory, Magnisense company for providing MIAtek.

1 U. Jeong, X. Teng, Y. Wang, H. Yang, Y. Xia, *Adv. Mater.* 2007 **19**, 33
2 F. M. Kievit , M.Zhang, *Acc. Chem. Res*. 2011 **44** , 853
3 S. Laurent, D. Forge, M. Port, A. Roch, C. Robic, L. V. Elst, and R. N. Muller, *Chem. Rev*. 2008 **108**, 2064
4 I. Milosevic, H. Jouni, C. David, F. Warmont, D. Bonnin, L. Motte, *J. Phys. Chem. C*. 2011, **115**, 18999
5 C. de Montferrand, L. Hu, I. Milosevic, V.Russier, D. Bonnin, L.Motte, A. Brioude, Y. Lalatonne *Acta Biomaterialia* 2013 **9**, 6150
6 J. Bolley, E. Guénin, N. Lievre, M. Lecouvey, M. Soussan, Y. Lalatonne, L. Motte *Langmuir* 2013 **29**, 14639
7 J. Baumgartner, A. Dey, P.H.H., Bomans, C. Coadou, P. Fratzl, N.A.J.M. Sommerdijk, D. Faivre, *Nat. Mater.*2013 **12**, 310
8 L. Vayssières, C. Chaneac, E. Tronc, J.P. Jolivet *J. Coll. Int. Sci.* 1998 **205**, 205
9 J.P. Jolivet, C. Froidefond, A. Pottier, C. Chanéac, S. Cassaignon, E. Tronc, P. Euzen *J. Mater. Chem.* 2004 **14**, 3281
10 U. Schwertmann, R. M. Cornell, Frontmatter, in Iron Oxides in the Laboratory: Preparation and Characterization Wiley-VCH Verlag GmbH, Weinheim, Germany 2007
11 M. Kallumadil, M. Tada, T. Nakagawa, M. Abe, P. Southern, Q.A. Pankhurst, *J. Magn. Magn. Mater.* 2009 **321**, 3650
12 J.P. Jolivet, Metal oxide chemistry and synthesis: from solution to solid state Wiley publisher, England 2000
13 R. M. Cornell, Schwertmann, U. The iron oxides Wiley-VCH Publishers, Weinheim, Germany, 2003
14 L. Lenglet, P. Nikitin, C. Pequignot, *POCT. IVD Technology* 2008 43
15 L. Motte, F. Benyettou, C. de Beaucorps, M. Lecouvey, I. Milosevic, Y.Lalatonne *Faraday Discuss.* 2011 **149**, 211
16 C. de Montferrand, Y. Lalatonne, D. Bonnin, N. Lièvre, M. Lecouvey, P. Monod, V. Russier, L. Motte, *Small* 2012 **8**, 1945
17 F. Geinguenaud, I. Souissi, R.Fagard, L. Motte, Y.Lalatonne, *Nanomedicine* 2012 **8**, 1106
18 F. Geinguenaud, I. Souissi, R. Fagard, Y. Lalatonne, L. Motte, L. *J. Phys. Chem. B* 2014 **118**, 1535
19 J.L. Dormann, D. Fiorani , E. Tronc, Adv. Chem. Phys. 1997 98, 283
20 X . Batlle, A. Labarta, *J. Phys. D.* 2002 **35**, R15
21 P. E. Jönsson, *Adv. Chem. Phys.* 2004 **128**, 191
22 J. Sun, S. Zhou, P. Hou, Y. Yang, J. Weng, X. H. Li ,M. Y. Li *J. Biomed. Mater. Res. A* 2007 **80**, 333
23 G. Gnanaprakash, S. Mahadevan, T. Jayakumar, P. Kalyanasundaram, J. Philip, B. Raj, *Mater. Chem. Phys*.2007 **103**, 168
24 M. Fang, V. Strom, R. . Olsson,L. Belova, K.V. Rao, *Appl. Phys. Lett.* 2011 **99**, 222501
25 C. Ravikumar, R Bandyopadhyaya *J. Phys. Chem. C* 2011 **115**, 1380
26 N.N. Song, H.T. Yang, X. Ren, Z.A.Li, Y. Luo, J. Shen, W.Dai, X.Q. Zhang, Z.H. Cheng *Nanoscale* 2013 **5**, 2804
27 M. P. Morales *Chem. Mater.* 1999 **11**, 3058
28 Y. Guyodo, S. K. Banerjee, R. Lee Penn, D.,Burleson, T. S. Berquo,T. Seda, P. Solheid, *Physics of the earth and planatory interiors* 2006 **154**, 222
29 J.R. Jeong, S.J. Lee, J.D. Kim, S.C. Shin, Phys Stat. sol. 2004 7, 1593